Shock metamorphic effects in the Ryugu carbonates

E. Dobrică[1], K. Nagashima[1], G. R. Huss[1], A. N. Krot[1] and A. J. Brearley[2]
[1]*Hawai'i Institute of Geophysics and Planetology, University of Hawai'i at Mānoa, HI, USA;* [2]*Department of Earth and Planetary Sciences, University of New Mexico, NM, USA.*

Introduction: Carbonates have traditionally been used to constrain the chemical evolution of fluids and the duration of aqueous alteration processes [1]. However, recent studies have shown that carbonates are also valuable recorders of shock metamorphic environments and help interpret shock metamorphic conditions on the chondrite parent asteroids [2-3]. Evidence of mild shock metamorphism, with an average peak pressure of ~2 GPa, has been reported in samples returned from the surface of the asteroid (162173) Ryugu by the JAXA Hayabusa2 spacecraft [4]. Only a small fraction of the material, around 0.2 vol%, experienced higher shock pressures exceeding 10 GPa during impact [5]. In this study, we focus on the effects of shock metamorphism on the carbonates identified in the Ryugu samples. Notably, three types of carbonates (calcite, dolomite, and magnesite) have been commonly observed in the main lithologies of Ryugu [6], with abundances reaching up to 4.4 vol% [5]. Calcite, though rare, has been identified in isolated clasts from chamber C, where it coexists with primary anhydrous silicate minerals such as Mg-rich olivine and pyroxene [7]. Isotopic measurements of oxygen and carbon indicate that most calcite precipitated first, followed by dolomite [7]. A key objective of our research is to determine whether carbonates formed from different fluid sources exhibit varying degrees of shock metamorphic alteration.

Samples and methods: We conducted an integrated study using scanning electron microscopy (SEM) and focused ion beam/transmission electron microscopy (FIB/TEM) to observe and analyze two Ryugu particles (A0104 and C0030), collected during the two touchdowns of the Hayabusa2 spacecraft in chambers A and C, respectively. We selected four regions containing the three different types of carbonates (calcite, dolomite, and Mn-rich magnesite) identified so far in the Ryugu samples for detailed analysis. The electron-transparent sections (three FIB sections from C0030 and one FIB section from A0104, designated A0104-026087) were prepared using the Helios 660 FIB-SEM instrument at the University of Hawai'i at Mānoa and examined by TEM using the JEOL NEOARM 200CF at the University of New Mexico.

Results and discussion: Our study reveals that two calcites from sample C0030 show no defects or evidence of shock metamorphism or space weathering (Fig. 1a, c-e). In contrast, the calcite from A0104 (Fig. 1b) exhibits radial dislocations throughout the crystal, many of which have split into partial dislocations [8], likely as a mechanism to reduce stress. This calcite is associated with Mg-rich olivine (Fo_{100}), similar to that described in less altered clasts by [7]. In general, all calcites display post-precipitation modifications, indicating interactions with fluids of varying compositions, both extraterrestrial and terrestrial. These alterations appear as heterogeneous, euhedral rims—either Mn-rich (Fig. 1b) or with calcium sulfate overgrowths up to 500 nm thick (Fig. 1a). The calcium sulfate likely formed within a relatively short timeframe, possibly less than a year of exposure to terrestrial conditions [9], despite the sample being stored in desiccators. Additionally, sodium-enriched regions (5.6 wt.% Na_2O) at the calcite grain boundary suggest later diffusion and further alteration after precipitation. This calcite is also associated with Mg- and Na-rich amorphous phosphate and Mn-rich magnesite [$Mg_{1.0}Mn_{0.8}Ca_{0.3}Fe_{0.3}(CO_3)_2$]. The Mn-rich magnesite exhibits modulations and strain contrast, possibly formed during crystal growth or shock metamorphism [3], and shows compositional heterogeneity with an FeO-rich rim and CaO-rich/CaO-poor zones (Fig. 1d-e).

We also prepared a FIB section of a large dolomite associated with other secondary phases such as apatite (Cl- and F-poor hydroxyapatite) and framboidal magnetite (Fig. 1f-g). In this section, two generations of dolomite were identified. The larger dolomite contains numerous pores and embayments, sometimes filled with phyllosilicates. Multiple signs of shock have been identified in this mineral, such as numerous dislocations, stacking faults, and parallel dislocations in multiple directions, similar to those observed in carbonates affected by shock metamorphism in CMs and Antarctic micrometeorites [2-3]. On the other hand, the smaller, euhedral dolomites (Fig. 1f) lack dislocations and were found in contact with large, anhedral apatites and dolomites. These observations indicate that the Ryugu samples were modified by multiple dissolution and precipitation events, and some of these events occurred after the shock processes, potentially as a result of the shock processes, as described by [10]. No space-weathering effects were observed in any dolomite or apatite crystals.

Our TEM observations demonstrate variability in the shock metamorphic effects among carbonates, indicating that not all carbonates were affected by the mild shock metamorphism described in previous studies [4]. Notably, the large dolomite crystal was the most significantly impacted by shock metamorphism. However, the absence of these shock features in certain

carbonate crystals implies their formation through multiple growth episodes facilitated by dissolution/precipitation processes. This suggests that some dolomites may have predated the formation of certain calcite crystals, a hypothesis that may be supported by distinct oxygen isotopic signatures among different calcite crystals [7].

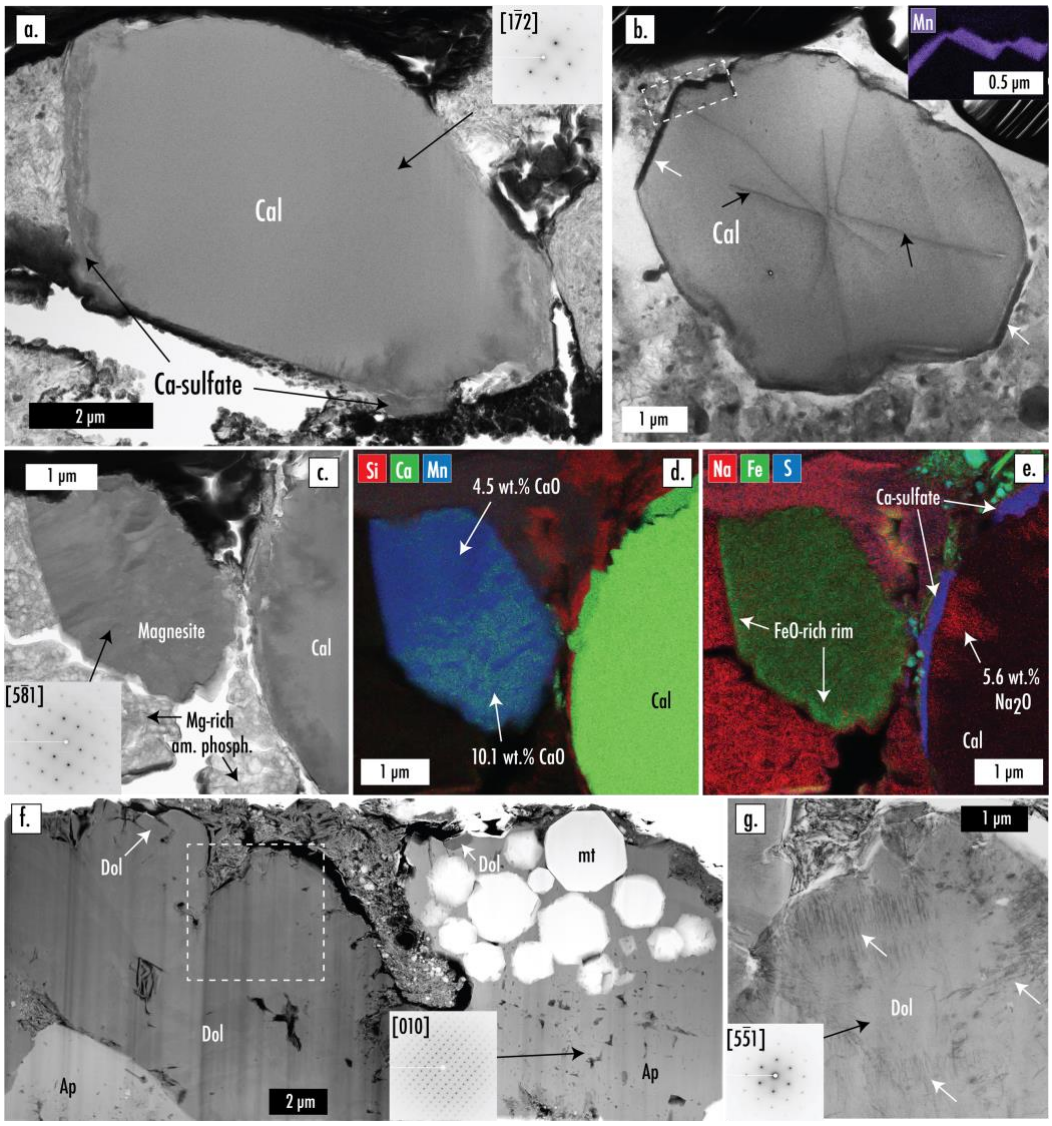

Figure 1. a) Nanobeam diffraction (NBD) image of calcite (Cal, [1-72] zone axis) showing no defects or space weathering effects. This calcite exhibits an overgrowth of calcium sulfates. b) NBD image of calcite from FIB section A0104-026087, revealing radial dislocations (black arrows) and a Mn-rich, heterogeneous euhedral rim (highlighted by white arrows and supported by the energy-dispersive X-ray spectroscopy (EDS) map, white dashed box from Fig. 1b: Mn – purple). c) NBD images of the Mn-rich magnesite associated with calcite and Mg-rich amorphous phosphate (Mg-rich am. phosph.). d-e) Composite EDS maps of Si, Ca, and Mn (d), and Na, Fe, and S (e), showing heterogeneities in calcite and the Mn-rich magnesite (from Fig. 1c). f) Dark-field scanning transmission electron microscopy (STEM) image of one of the FIB sections prepared at the boundary between the large dolomite (Dol) and apatite (Ap, [010] zone axis). Framboidal magnetite (mt) is embedded within the porous apatite. Small (~1 µm in length) euhedral dolomites are indicated by white arrows (from Fig. 1f). g) NBD image of the dolomite crystal ([5-51] zone axis, white dashed box from Fig. 1f) containing numerous defects (see white arrows) produced through shock metamorphism.

References

[1] Tyra M. et al. (2012) *Geochimica et Cosmochimica Acta*, 77:383-395. [2] Dobrică E. et al. (2024) *Geochimica et Cosmochimica Acta*, 368:112–125. [3] Dobrică E. et al. (2022) *Geochimica et Cosmochimica Acta*, 317:286-305. [4] Tomioka N. (2023) *Nature Astronomy*, 7:669-677. [5] Nakamura T. et al. (2022) *Science*, 10.1126/science.abn8671. [6] Kawasaki N. et al. (2022) *Science Advances*, 8:eade2067. [7] Fujiya W. et al. (2023) *Nature Geoscience*, 16:675-682. [8] Shih M. et al. (2021) *Nature Communications*, 12:3590. [9] Gounelle M. and Zolensky M. E. (2001) *Meteoritics & Planetary Science*, 36:1321-1329. [10] Rubin A. E. (2012) *Geochimica et Cosmochimica Acta*, 90:181-194.